



Elasticity Solution Approach for Functionally Graded Spherical Shell with Piezoelectric Properties

In this paper, an analytical method is adopted, based on elasticity approach to analyze the hollow FGM sphere with piezoelectric properties. The electro-mechanical properties except the Poisson's ratio are assumed to be power functions of radius. Loading is a combination of pressures and a distributed electric field. For axisymmetric problem, 3-D governing equations are reduced to a 1-D second order nonlinear Cauchy-type differential equation, in terms of radial displacement. The solution of nonlinear differential equation is opted as a power law function. By satisfying five sets of boundary conditions and incorporating them into governing equation, a system of algebraic equations is obtained that delivers the unknown constants. Static responses of FG shell to electro-mechanical loads with different 'n' and the effect of size are investigated. The induced radial and circumferential stresses of an imposed electric potential are compared to the residual stresses locked in the homogeneous sphere.

MR. Saviz*
Assistant Professor

A. Ghorbanpour Arani*
Professor

Keywords: Functionally graded material; Piezoelectric material; Sphere; Elasticity solution; Nonlinear differential equation.

1 Introduction

Piezoelectric materials have been widely used as distributed sensors and actuators in the field of smart structures and active structural control. A smart structure typically comprises of one or more active (or functional) materials. The lightweight high-strength shells with piezoelectric properties are famous for their capability of providing the expected behaviour at the smart structures level. Crawley [1] reported an overview of applications of piezoelectric materials for intelligent and aerospace structures. Functionally graded materials (FGMs) are microscopically inhomogeneous composites usually made from a mixture of metals and ceramics. By gradually varying the volume fraction of consistent materials, their material properties exhibit a smooth and continuous change along one or more directions to obtain optimum response to externally applied loads.

*Corresponding Author, Assistant Professor, Mechanical Engineering Department, Azarbaijan Shahid Madani University, Tabriz, Iran, saviz@azaruniv.ac.ir

† Professor, Department of Mechanical Engineering, University of Kashan, Kashan, Iran, ghorbanpor@yahoo.com

Niino [2] introduced the concept of functionally graded material to satisfy the demand of ultra-high-temperature environment and to eliminate the stress singularities. Yamada et al. [3] presented a functionally graded piezoelectric plate created by forming a temperature variation across the plate with relatively low Curie temperature. Chen et al. [4] presented the static analysis of a steadily rotating piezoelectric spherical shell with a functionally graded property. Electromechanical responses of compositionally graded piezoelectric layers were analysed by Lim and He [5]. Sinha [6] obtained the solution of the problem of static radial deformation of a piezoelectric spherical shell and under a given voltage difference between these surfaces, coupled with a radial distribution of temperature from the inner to the outer surface. Three-dimensional elasticity static analysis of a multilayered elastic spherical hollow shell with spherical isotropy was presented by Chen and Ding [7].

Two independent state equations were derived after introducing three displacement functions and two stress functions. Ghorbanpour et al. [8] investigated the stress and electric potential fields in piezoelectric hollow spheres. The stress field in piezoelectric hollow sphere under thermal environment was developed by Saadatfar and Rastgoo [9]. Shao et al. [10] derived analytical solutions for mechanical stresses of a functionally graded circular hollow cylinder with finite length. In-homogeneity was considered in a number of studies. Elastic analysis of internally pressurized thick-walled spherical pressure vessels of functionally graded materials (FGMs) investigated by You et al. [11]. Sladek et al. [12] derived Local integral equations for numerical solution of 3-D problems in linear elasticity of FGMs viewed as 2-D axisymmetric problems. The meshless local Petrov–Galerkin method was applied to transient dynamic problems in 3D axisymmetric piezoelectric solids with continuously non-homogeneous material properties subjected to mechanical and thermal loads by Sladek et al. [13]. Wang and Xu [14] studied the effect of material inhomogeneity on electromechanical behaviors of functionally graded piezoelectric spherical structures. Magneto-thermoelastic problems of FGM spheres are studied by Ghorbanpour et al. [15].

Transient analysis of ordinary functionally graded cylindrical shells subjected to internal dynamic pressure was presented by Setoodeh et al. [16], implementing a power law distribution function in the thickness. Ghorbanpour Arani et al. [17] solved hollow sphere made from functionally graded piezoelectric material, using unnecessary dimensionless quantities. They considered a particular solution, not satisfying the governing equation and an exponential function for general solution of Cauchy-Euler equation, instead of a power law function, which is given in mathematical Handbooks (e.g. [18]). Buckling of shallow functionally graded spherical shells with surface-bonded piezoelectric actuators under thermal load was studied by Sabzikar Boroujerdy and Eslami [19]. It was assumed that properties of the functionally graded material vary through the thickness according to a power law distribution of the volume fractions of the constituent materials. The static and dynamic responses of a simply-supported, thick laminated orthotropic cylindrical shell with piezoelectric actuator and sensor layers, based on a 3-D elasticity solution approach was published by Shakeri et al. [20]. Hafezalkotob and Eslami [21] presented the thermo-mechanical buckling of simply supported thin shallow spherical shells made of functionally graded material. In this paper, the first-order shell theory of Love and Kirchhoff, the Donnell-Mushtari-Vlasov kinematics equations, and the calculus of variations was used.

Therefore, in conjunction with the previous works, new applications of piezoelectric sensors and actuators are being introduced for a new geometric configuration. This research attempts to analyse a hollow sphere composed of a radially polarized transversely isotropic functionally graded piezoelectric material, subjected to uniform static load together with a potential difference induced by electrodes attached to the inner and outer surfaces of the annular sphere.

All mechanical and piezoelectric properties of the FGM hollow sphere, except for the Poisson's ratio, are assumed to depend on the radius r and expressed in terms of its power function with material in-homogeneity level ' n '. The 3-D governing equilibrium equations of radially polarized sphere are reduced to a system of second-order ordinary differential equations, yielding a 1-D second order nonlinear Cauchy-type differential equation in terms of radial displacement, which then is solved analytically. By satisfying four different sets of boundary conditions and incorporating them into governing equation, a system of algebraic equations is obtained that delivers the unknown constants. The accuracy and computational efficiency of the proposed approach are verified by comparing the results with those obtained for homogenous material in the literature.

2 Formulation and theory

Consider a hollow FGPM sphere with inside radius R_i , outside radius R_o , and total shell thickness H . The shell geometry exposed to uniform internal and external pressures P_i and P_o , and distributed electric potential V is shown in Figure (1). Because of the closed geometry, the electrodes have to be attached to the outer and inner surfaces during the manufacturing process. This leads to having an electric field in radial direction. Furthermore, the direction of polarization is established during the induction process by means of the electric field applied between two electrodes and its quantity is determined by electric displacement. So, in a thickness-wise polarized piezoelectric sphere, there will be only radial components of electric field and displacement. Details with respect to definition and determination of the constants describing these materials have been standardized by the Institute of Electrical and Electronics Engineers [22]. For centre-symmetric stress and displacement conditions, the linear constitutive relations for an orthotropic material, with radially polarized piezoelectric property can be written as follows, [23], [24]:

$$\begin{Bmatrix} \sigma_r \\ \sigma_\theta \\ \sigma_\phi \end{Bmatrix} = \begin{bmatrix} c_{11} & c_{12} & c_{13} \\ c_{21} & c_{22} & c_{23} \\ c_{31} & c_{32} & c_{33} \end{bmatrix} \begin{Bmatrix} \varepsilon_r \\ \varepsilon_\theta \\ \varepsilon_\phi \end{Bmatrix} - EF_r \begin{Bmatrix} e_{11} \\ e_{12} \\ e_{13} \end{Bmatrix} \quad (1-a)$$

$$ED_r = \begin{bmatrix} e_{11} & e_{12} & e_{13} \end{bmatrix} \begin{Bmatrix} \varepsilon_r \\ \varepsilon_\theta \\ \varepsilon_\phi \end{Bmatrix} + \Delta_{11} E_r \quad (1-b)$$

Where c_{ij} , Δ_{ij} , and e_{ij} are the elastic, dielectric, and piezoelectric constants, respectively, which relate the components of stress (σ), strain (ε), electric field (EF) and electric displacement vectors (ED). It is assumed that the functionally graded material has transversely isotropic properties with respect to axis of rotation oriented in the radial direction, the elasticity and piezoelectric coefficient tensors are expressed as

$$c_{12} = c_{21} = c_{13} = c_{31}, \quad c_{22} = c_{33}, \quad c_{32} = c_{23}, \quad e_{12} = e_{13} \quad (2-a)$$

Hence, it has only three independent material parameters, in addition to a piezoelectric coefficient. In case of having the mechanical properties (directional elastic moduli and poisson's ratios), by using micro-mechanics, rule of mixtures or experiment, the elastic coefficients for thickness-wise FGM sphere are obtained as follows, [23]

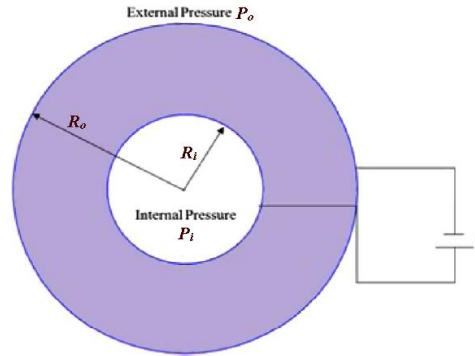


Figure 1 FGPM shell geometry subject to uniform pressure and applied voltage.

$$c_{11}(r) = \frac{E_{11}(r)(1-\nu_{23}^2)}{1-\nu_{23}^2-2\nu_{12}\nu_{21}(1+\nu_{23})}, \quad c_{22}(r) = c_{33}(r) = \frac{E_{22}(r)(1-\nu_{12}\nu_{21})}{1-\nu_{23}^2-2\nu_{12}\nu_{21}(1+\nu_{23})}, \quad (2-b)$$

$$c_{12}(r) = c_{13}(r) = \frac{E_{22}(r)\nu_{12}(1+\nu_{23})}{1-\nu_{23}^2-2\nu_{12}\nu_{21}(1+\nu_{23})}, \quad c_{23}(r) = \frac{E_{22}(r)(\nu_{23}+\nu_{12}\nu_{21})}{1-\nu_{23}^2-2\nu_{12}\nu_{21}(1+\nu_{23})}$$

where, Poisson's ratio is assumed to be constant through the shell thickness. For isotropic properties, the FGM elastic coefficients are summarized to the following relations, [7]

$$c_{11}(r) = c_{22}(r) = c_{33}(r) = \frac{(1-\nu)E(r)}{(1+\nu)(1-2\nu)}, \quad (2-c)$$

$$c_{12}(r) = c_{21}(r) = c_{13}(r) = c_{31}(r) = c_{23}(r) = c_{32}(r) = \frac{\nu E(r)}{(1+\nu)(1-2\nu)}$$

The centre-symmetric equations of motion ($\frac{\partial}{\partial \theta} = \frac{\partial}{\partial \phi} = 0$) in the absence of body force are

$$\frac{\partial \sigma_r}{\partial r} + \frac{2\sigma_r - \sigma_\theta - \sigma_\phi}{r} = 0 \quad (3-a)$$

The charge equation of electrostatics is given by Tiersten [24].

$$\frac{\partial ED_r}{\partial r} + \frac{2ED_r}{r} = 0 \quad (3-b)$$

The centre-symmetric strain-displacement and the electric field-electric potential relations of the piezoelectric elastic medium are written as

$$\varepsilon_r = \frac{\partial u_r}{\partial r}, \quad \varepsilon_\phi = \frac{u_r}{r}, \quad \varepsilon_\theta = \frac{u_r}{r}, \quad (4-a)$$

$$EF_r = -\frac{\partial \psi}{\partial r} \quad (4-b)$$

By combining Eqs. (4) with Eqs. (1), the stress and electrical displacement component will be obtained as follows

$$\sigma_r = c_{11} \frac{\partial u_r}{\partial r} + (c_{12} + c_{13}) \left(\frac{u_r}{r} \right) + e_{11} \frac{\partial \psi}{\partial r}$$

$$\sigma_\theta = c_{12} \frac{\partial u_r}{\partial r} + (c_{22} + c_{23}) \left(\frac{u_r}{r} \right) + e_{12} \frac{\partial \psi}{\partial r} \quad (5-a)$$

$$\sigma_z = c_{13} \frac{\partial u_r}{\partial r} + (c_{23} + c_{33}) \left(\frac{u_r}{r} \right) + e_{13} \frac{\partial \psi}{\partial r}$$

$$ED_r = e_{11} \frac{\partial u_r}{\partial r} + (e_{12} + e_{13}) \left(\frac{u_r}{r} \right) - A_{11} \frac{\partial \psi}{\partial r} \quad (5-b)$$

After substituting these components into the governing Eqs. (3) and factorizing the similar derivatives of u_r and ψ , the equations of equilibrium in terms of displacement and electric potential for spherical shell become:

$$c_{11}(r) \frac{\partial^2 u_r}{\partial r^2} + \left(\frac{2c_{11}(r)}{r} + \frac{dc_{11}(r)}{dr} \right) \frac{\partial u_r}{\partial r} + \frac{2}{r} \left(\frac{dc_{12}(r)}{dr} - \frac{c_{23}(r) + c_{22}(r) - c_{12}(r)}{r} \right) u_r + e_{11}(r) \frac{\partial^2 \psi}{\partial r^2} + \left(\frac{2(e_{11}(r) - e_{12}(r))}{r} + \frac{de_{11}(r)}{dr} \right) \frac{\partial \psi}{\partial r} = 0 \quad (6-a)$$

$$e_{11}(r) \frac{\partial^2 u_r}{\partial r^2} + \left(\frac{2(e_{11}(r) + e_{12}(r))}{r} + \frac{de_{11}(r)}{dr} \right) \frac{\partial u_r}{\partial r} + \frac{2}{r} \left[\frac{de_{12}(r)}{dr} + \frac{e_{12}(r)}{r} \right] u_r - A_{11}(r) \frac{\partial^2 \psi}{\partial r^2} - \left[\frac{dA_{11}(r)}{dr} + \frac{2A_{11}(r)}{r} \right] \frac{\partial \psi}{\partial r} = 0 \quad (6-b)$$

For isotropic FG material, the mechanical equation of motion is simplified as

$$c_{11}(r) \frac{\partial^2 u_r}{\partial r^2} + \left(\frac{2c_{11}(r)}{r} + \frac{dc_{11}(r)}{dr} \right) \frac{\partial u_r}{\partial r} + \frac{2}{r} \left(\frac{dc_{12}(r)}{dr} - \frac{c_{11}(r)}{r} \right) u_r + e_{11}(r) \frac{\partial^2 \psi}{\partial r^2} + \left(\frac{2(e_{11}(r) - e_{12}(r))}{r} + \frac{de_{11}(r)}{dr} \right) \frac{\partial \psi}{\partial r} = 0$$

By substituting components of the elastic constants from the above equations (2) into Eq. (6-a), the equilibrium equation is developed in terms of the displacement and electric potential field of the functionally graded spherical shell, while the electrical equilibrium Eq. (6-b) remains the same, as follows:

$$\frac{E(r)(\nu - 1)}{(1 + \nu)(1 - 2\nu)} \left(\frac{\partial^2 u_r}{\partial r^2} + \frac{2}{r} \frac{\partial u_r}{\partial r} - \frac{2}{r^2} u_r \right) + \frac{1}{(1 + \nu)(1 - 2\nu)} \left((\nu - 1) \frac{\partial u_r}{\partial r} - 2\nu u_r \right) \frac{dE(r)}{dr} + e_{11}(r) \frac{\partial^2 \psi}{\partial r^2} + \left(\frac{e_{11}(r) - 2e_{12}(r)}{r} + \frac{de_{11}(r)}{dr} \right) \frac{\partial \psi}{\partial r} = 0 \quad (7)$$

On the other hand, the FGM properties change through the r -direction, which can be a combination of ceramics and metals. The mixing ratio is varied continuously and smoothly across the thickness. The following model is taken for material property distribution [13], [19]

$$q(r) = q_i \left(\frac{r}{R_i} \right)^n \quad (8)$$

$q(r)$ is material property that is controlled by volume fraction as a function of r , ' n ' is the none-negative power-law exponent and subscripts i and o stand for inner and outer surfaces. $q(r)$ can be substituted for Young's modulus $E(r)$, shear modulus $G(r)$, electric coefficients $e_{11}(r)$, $e_{12}(r)$ and mass density $\rho(r)$. Poisson's ratio is considered constant through the thickness. Variation of material properties in terms of volume fraction of external / interior material with normalized radial distance in thickness direction for different values of n are shown in Figure (2).

2.1 Boundary conditions

Because of symmetric geometry, there is no essential boundary condition in this problem. The loading condition of the outer/ inner surface of the shell is considered to be free of shear/ in plane traction and the electro-static potential is assumed to be zero on the outer surface. Under these circumstances, four sets of mechanical and electrical loading boundary conditions of the FGP sphere are written as follows:

$$\text{I) } \sigma_r(R_i) = P_i, \quad \sigma_r(R_o) = 0, \quad \psi(R_i) = 0, \quad \psi(R_o) = 0 \quad (9\text{-a})$$

$$\text{II) } \sigma_r(R_i) = 0, \quad \sigma_r(R_o) = 0, \quad \psi(R_i) = V_i, \quad \psi(R_o) = 0 \quad (9\text{-b})$$

$$\text{III) } \sigma_r(R_i) = 0, \quad \sigma_r(R_o) = P_o, \quad \psi(R_i) = 0, \quad \psi(R_o) = 0 \quad (9\text{-c})$$

$$\text{IV) } \sigma_r(R_i) = P_i, \quad \sigma_r(R_o) = 0, \quad \psi(R_i) = V_i, \quad \psi(R_o) = 0 \quad (9\text{-d})$$

$$\text{V) } \sigma_r(R_i) = P_i, \quad \sigma_r(R_o) = 0, \quad \psi(R_i) = 0, \quad \psi(R_o) = V_o \quad (9\text{-e})$$

In case I, the FGPM hollow sphere is subjected to an internal uniform pressure without any imposed electric potential and external pressure. However, in this case the induced electric potential is existed across the thickness. In this case, the sphere acts as a sensor. In the second case, an electrical potential difference is applied between the inner and outer surfaces of the sphere without any internal and external pressures. In this case, the sphere acts as an actuator. In case III, the FGPM hollow sphere is exposed to an external uniform pressure without any imposed electric potential and internal pressure. Cases IV and V are the superposition of cases I and II, along with an electrical potential on the external electrode on the shell surface.

3 Analytical solution method

The trivial solution of electric equilibrium Eq. (3-b) is as follows, [17]

$$ED_r(r) = \frac{D}{r^2} \quad (10)$$

where, D is an unknown constant that should be determined using boundary conditions. Using this solution, combining equations (6-a) and (6-b) and collecting the similar derivatives of radial displacement, yields as follows

$$\begin{aligned} & \left(c_{11}(r) + \frac{e_{11}^2(r)}{A_{11}(r)} \right) \frac{\partial^2 u_r}{\partial r^2} + \left(\frac{dc_{11}(r)}{dr} + \frac{e_{11}(r)}{A_{11}(r)} \left\{ 2 \frac{de_{11}(r)}{dr} - \frac{e_{11}(r)}{A_{11}(r)} \frac{dA_{11}(r)}{dr} \right\} \right) \frac{\partial u_r}{\partial r} \\ & + \frac{2}{r} \frac{e_{11}^2(r) + c_{11}(r)A_{11}(r)}{A_{11}(r)} \\ & + \frac{2}{r^2} \left(c_{12}(r) - c_{23}(r) - c_{22}(r) + \frac{e_{11}(r)}{A_{11}(r)} \left\{ e_{12}(r) + r \frac{de_{12}(r)}{dr} \right\} - 2 \frac{e_{12}^2(r)}{A_{11}(r)} + r \frac{dc_{12}(r)}{dr} \right. \\ & \left. + r \frac{e_{12}(r)}{A_{11}(r)} \frac{de_{11}(r)}{dr} - r \frac{e_{12}(r)e_{11}(r)}{A_{11}^2(r)} \frac{dA_{11}(r)}{dr} \right) u_r \\ & + \frac{D}{r^2} \left(\frac{e_{11}(r)}{A_{11}^2(r)} \frac{dA_{11}(r)}{dr} - \frac{1}{A_{11}(r)} \frac{de_{11}(r)}{dr} + \frac{2}{r} \frac{e_{12}(r)}{A_{11}(r)} \right) = 0 \end{aligned} \quad (11\text{-a})$$

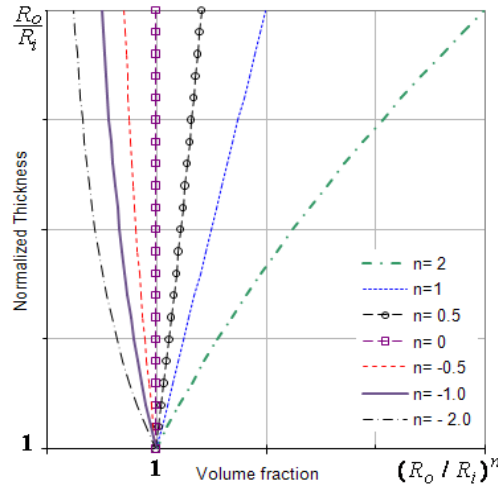


Figure 2 Material property variation in terms of exponent n

For isotropic FG material, the mechanical static equilibrium is simplified as

$$\begin{aligned}
 & \left(\frac{E(r)(1-\nu)}{(1+\nu)(1-2\nu)} - \frac{e_{11}^2(r)}{\Delta_{11}(r)} \right) \frac{\partial^2 u_r}{\partial r^2} + \left(\frac{2}{r} \left\{ \frac{(1-\nu)}{(1+\nu)(1-2\nu)} \left[E(r) - \frac{r}{2} \frac{dE(r)}{dr} \right] - \frac{e_{11}^2(r)}{\Delta_{11}(r)} \right\} \right. \\
 & \left. + \frac{e_{11}^2(r)}{\Delta_{11}^2(r)} \frac{d\Delta_{11}(r)}{dr} - 2 \frac{e_{11}(r)}{\Delta_{11}(r)} \frac{de_{11}(r)}{dr} \right) \frac{\partial u_r}{\partial r} \\
 & + \frac{2}{r^2} \left(\frac{e_{12}^2(r)}{\Delta_{11}(r)} - \frac{1}{(1+\nu)(1-2\nu)} \left[E(r)(1-\nu) + r\nu \frac{dE(r)}{dr} \right] - \frac{e_{11}(r)e_{12}(r)}{\Delta_{11}(r)} \right) \\
 & \left. - r \left\{ \frac{e_{11}(r)}{\Delta_{11}(r)} \frac{de_{12}(r)}{dr} + \frac{e_{12}(r)}{\Delta_{11}(r)} \frac{de_{11}(r)}{dr} - \frac{e_{11}(r)e_{12}(r)}{\Delta_{11}^2(r)} \frac{d\Delta_{11}(r)}{dr} \right\} \right) u_r \\
 & + \frac{D}{r^2} \left(\frac{e_{11}(r)}{\Delta_{11}^2(r)} \frac{d\Delta_{11}(r)}{dr} - \frac{1}{\Delta_{11}(r)} \frac{de_{11}(r)}{dr} + \frac{2}{r} \frac{e_{12}(r)}{\Delta_{11}(r)} \right) = 0
 \end{aligned} \tag{11-b}$$

At this stage, the elasticity and electricity coefficients are obtained from Eq.(8)

$$c_{ij}(r) = C_{ij}(r/R_i)^n, E(r) = E(r/R_i)^n, e_{11}(r) = e_{11}(r/R_i)^n, e_{12}(r) = e_{12}(r/R_i)^n, \Delta_{11}(r) = \Delta_{11}(r/R_i)^n \tag{12-a}$$

The Poisson's ratios (ν_{ij}) are assumed constant in different directions.

$$\text{where, } C_{11} = \frac{E_{11}(1-\nu_{23}^2)}{1-\nu_{23}^2-2\nu_{12}\nu_{21}(1+\nu_{23})}, C_{12} = \frac{E_{22}\nu_{12}(1+\nu_{23})}{1-\nu_{23}^2-2\nu_{12}\nu_{21}(1+\nu_{23})}, \tag{12-b}$$

$$\text{for isotropic case: } C_{11} = \frac{(1-\nu)E}{(1+\nu)(1-2\nu)}, C_{12} = \frac{\nu E}{(1+\nu)(1-2\nu)}$$

By substituting Eqs. (12) into Eq. (11-a), the following non-linear partial differential equation emerges

$$\begin{aligned}
& r^n \left(C_{11} + \frac{e_{11}^2}{\Delta_{11}} \right) \frac{\partial^2 u_r}{\partial r^2} + \frac{r^n}{r} \left(\left(C_{11} + \frac{e_{11}^2}{\Delta_{11}} \right) (2+n) \right) \frac{\partial u_r}{\partial r} \\
& + \frac{2r^n}{r^2} \left(C_{12}(1+n) - C_{22} - C_{23} + (1+n) \frac{e_{11}e_{12}}{\Delta_{11}} - 2 \frac{e_{12}^2}{\Delta_{11}} \right) u_r + \frac{2D}{r^3} \left(\frac{e_{12}}{\Delta_{11}} \right) = 0
\end{aligned} \tag{13-a}$$

For isotropic FG material, the non-linear partial differential equation is written as

$$\begin{aligned}
& r^n \left(\frac{E(1-\nu)}{(1+\nu)(1-2\nu)} + \frac{e_{11}^2}{\Delta_{11}} \right) \frac{\partial^2 u_r}{\partial r^2} + r^n \frac{1}{r} \left(\frac{(1-\nu)E(2+n)}{(1+\nu)(1-2\nu)} + \frac{e_{11}^2}{\Delta_{11}} (2+n) \right) \frac{\partial u_r}{\partial r} \\
& + r^n \frac{2}{r^2} \left(\frac{E}{(1+\nu)(1-2\nu)} [\nu(1+n) - 1] + (1+n) \frac{e_{11}e_{12}}{\Delta_{11}} - 2 \frac{e_{12}^2}{\Delta_{11}} \right) u_r + \frac{2D}{r^3} \left(\frac{e_{12}}{\Delta_{11}} \right) = 0
\end{aligned} \tag{13-b}$$

Multiplying Eq.(13-a) with $r^{(2-n)}$, yields a non-homogeneous Cauchy-Euler type differential equation as follows

$$r^2 \frac{\partial^2 u_r}{\partial r^2} + \gamma_1 r \frac{\partial u_r}{\partial r} + \gamma_2 u_r = -\gamma_3 D r^{-(n+1)} \tag{14}$$

where,

$$\begin{aligned}
\gamma_1 &= (2+n) \\
\gamma_2 &= 2 \frac{(C_{12}(1+n) - C_{22} - C_{23})\Delta_{11} + (1+n)e_{11}e_{12} - 2e_{12}^2}{C_{11}\Delta_{11} + e_{11}^2} \\
\gamma_3 &= \frac{2e_{12}}{C_{11}\Delta_{11} + e_{11}^2}
\end{aligned} \tag{15-a}$$

For isotropic FG material, these multipliers are

$$\begin{aligned}
\gamma_1 &= (2+n) \\
\gamma_2 &= 2 \frac{E \Delta_{11} [\nu(1+n) - 1] + (1+\nu)(1-2\nu) \left((1+n)e_{11}e_{12} - (1+2n)e_{12}^2 \right)}{E \Delta_{11} (1-\nu) + (1+\nu)(1-2\nu) e_{11}^2} \\
\gamma_3 &= \frac{2e_{12}(1+\nu)(1-2\nu)}{E \Delta_{11} (1-\nu) + (1+\nu)(1-2\nu) e_{11}^2}
\end{aligned} \tag{15-b}$$

The general solution for Eq. (14) has the following well known form, [18]:

$$u_{rg} = u_{rg1} + u_{rg2} = K_1 r^{\lambda_1} + K_2 r^{\lambda_2} \tag{16}$$

$$\text{where } \lambda_{1,2} = \frac{1 - \gamma_1 \pm \sqrt{(\gamma_1 - 1)^2 - 4\gamma_2}}{2}$$

Subsequently, the particular solution of Eq. (14) can be developed by employing the method, so called variation of parameter [18], as

$$u_{rp} = R_1(r) u_{rg1} + R_2(r) u_{rg2} \tag{17}$$

R_1 and R_2 can be determined by substituting Eq. (17) into equilibrium Eq. (14) as

$$\begin{aligned}
R_1(r) &= \int F(r) u_{rg2} dr, & R_2(r) &= -\int F(r) u_{rg1} dr \\
F(r) &= \frac{W(r)}{\kappa(\lambda_1, \lambda_2)}, & \kappa &= u_{rg1} \frac{du_{rg2}}{dr} - u_{rg2} \frac{du_{rg1}}{dr}
\end{aligned} \tag{18}$$

Where $W(r)$ is the expression on the right hand side of Eq. (14). Substituting Eq. (18) into Eq. (17), the overall solution is found as follows

$$u_r = K_1 r^{\lambda_1} + K_2 r^{\lambda_2} - \frac{\gamma_3 D}{(n+1)(n+2) - \gamma_1(n+1) + \gamma_2} r^{-n-1} \tag{19}$$

Where K_1, K_2 are unknown constants that are determined using boundary conditions. Now, by substituting the displacement from Eq. (19) into Eqs. (5) the radial stress is obtained. Also, substituting u_r into Eq. (5-b), then combining with Eq. (4-b) and performing integration, electric potential along with radial stress are written as

$$\begin{Bmatrix} \sigma_r(r) \\ \psi(r) \end{Bmatrix} = \begin{bmatrix} A_{11}(r) & A_{12}(r) & A_{13}(r) & 0 \\ A_{21}(r) & A_{22}(r) & A_{23}(r) & 1 \end{bmatrix} \begin{Bmatrix} K_1 \\ K_2 \\ D \\ C' \end{Bmatrix} \tag{20-a}$$

$$\begin{aligned}
A_{11}(r) &= \frac{1}{\Delta_{11}} \left[(C_{11}\Delta_{11} + e_{11}^2)\lambda_1 + 2(C_{12}\Delta_{11} + e_{11}e_{12}) \right] r^{\lambda_1+n-1} \\
A_{12}(r) &= \frac{1}{\Delta_{11}} \left[(C_{11}\Delta_{11} + e_{11}^2)\lambda_2 + 2(C_{12}\Delta_{11} + e_{11}e_{12}) \right] r^{\lambda_2+n-1} \\
A_{13}(r) &= \frac{1}{\Delta_{11}} \left(\frac{\gamma_3 \left[(C_{11}\Delta_{11} + e_{11}^2)(1+n) - 2(C_{12}\Delta_{11} + e_{11}e_{12}) \right]}{(n+1)(n+2) - \gamma_1(n+1) + \gamma_2} - e_{11} \right) r^{-2} \\
A_{21}(r) &= \frac{1}{\Delta_{11}} \left(e_{11} - \frac{2e_{12}}{\lambda_1} \right) r^{\lambda_1} \\
A_{22}(r) &= \frac{1}{\Delta_{11}} \left(e_{11} - \frac{2e_{12}}{\lambda_2} \right) r^{\lambda_2} \\
A_{23}(r) &= \frac{1}{\Delta_{11}} \left(1 - \frac{\gamma_3 [e_{11}(n+1) + 2e_{12}]}{(n+1)(n+2) - \gamma_1(n+1) + \gamma_2} \right) \frac{r^{-n-1}}{n+1}
\end{aligned} \tag{20-b}$$

C' is the integration constant. For all the four load cases mentioned in boundary conditions, the system of linear algebraic equations for the constants K_1, K_2, D and C' of Eqs. (20) can be written in the following from

$$\begin{Bmatrix} K_1 \\ K_2 \\ D \\ C' \end{Bmatrix} = \begin{bmatrix} A_{11}(R_i) & A_{21}(R_i) & A_{13}(R_i) & 0 \\ A_{11}(R_o) & A_{12}(R_o) & A_{13}(R_o) & 0 \\ A_{21}(R_i) & A_{22}(R_i) & A_{23}(R_i) & 1 \\ A_{21}(R_o) & A_{22}(R_o) & A_{23}(R_o) & 1 \end{bmatrix}^{-1} \begin{Bmatrix} \sigma_r(R_i) \\ \sigma_r(R_o) \\ \psi(R_i) \\ \psi(R_o) \end{Bmatrix} \tag{21}$$

The components of vector on the right side are defined in boundary condition Eqs. (9). Once the vector of constants is calculated, by using Eqs. (19) and (20) the displacement, electric potential and stress would be obtained. Consequently, the circumferential stress is calculated by using the following relation

$$\begin{aligned} \sigma_{\theta}(r) = & \frac{K_1}{\Delta_{11}} \left[(C_{12}\Delta_{11} + e_{11}e_{12})\lambda_1 + (C_{22} + C_{23})\Delta_{11} + 2e_{12}^2 \right] r^{\lambda_1+n-1} \\ & + \frac{K_2}{\Delta_{11}} \left[(C_{12}\Delta_{11} + e_{11}e_{12})\lambda_2 + (C_{22} + C_{23})\Delta_{11} + 2e_{12}^2 \right] r^{\lambda_2+n-1} \\ & + \frac{D}{\Delta_{11}} \left(\frac{\gamma_3 \left[(C_{12}\Delta_{11} + e_{11}e_{12})(1+n) - (C_{22} + C_{23})\Delta_{11} - 2e_{12}^2 \right]}{(n+1)(n+2) - \gamma_1(n+1) + \gamma_2} - e_{12} \right) r^{-2} \end{aligned} \quad (22)$$

4 Evaluation and Numerical results

The effectiveness of the developed formulation has been demonstrated through the analysis of examples and making comparisons with the published results in benchmark problems. In the first step, a spherical shell with $R_o/R_i = 2$, and made of homogenous isotropic material with the following steel-like properties is considered, while putting the piezoelectric related constants equal to a negligible value: $E = 207$ GPa, $\nu = 0.29$. The shell is subjected to an external uniform pressure (load case III). In Figures 3(a) and (b) the distributions of the non-dimensional radial stress σ_r / P_o and normalized radial displacement $u_r E / (2(1+\nu)R_o P_o)$, respectively are compared to the results obtained by Chen and Ding [7]. Secondly, the following transversely isotropic shell is investigated:

Shell A) Spherical shell made of piezoelectric ceramic PZT-5 with the material properties given in Table (1), [8]. In the first step, the results obtained for four different static loadings of shell A are compared to the reported results [8].

Three geometrical properties of the symmetric sphere are considered: $R_o/R_i = 1.3, 2.4$ and 4.0 . In Table (2), the values of radial stress, circumferential stress and electric potential on the mid-radius of the shell $((R_o / R_i)/2)$ are compared to those obtained by Ghorbanpour et al. [8]. Without surprise, it is seen that there is a good agreement between the present results and the reported ones. The reasons for these differences are dissimilar formulation and computational approach. In the present work, the Maple software has been implemented to solve the governing equations in parametrical form, consuming less time and computational effort. It is seen that the present approach, to some extent overestimates the results. Having done the aforementioned study, the capability of the proposed formulation and developed computer code to analyse the FGPM spherical shell has been assessed.

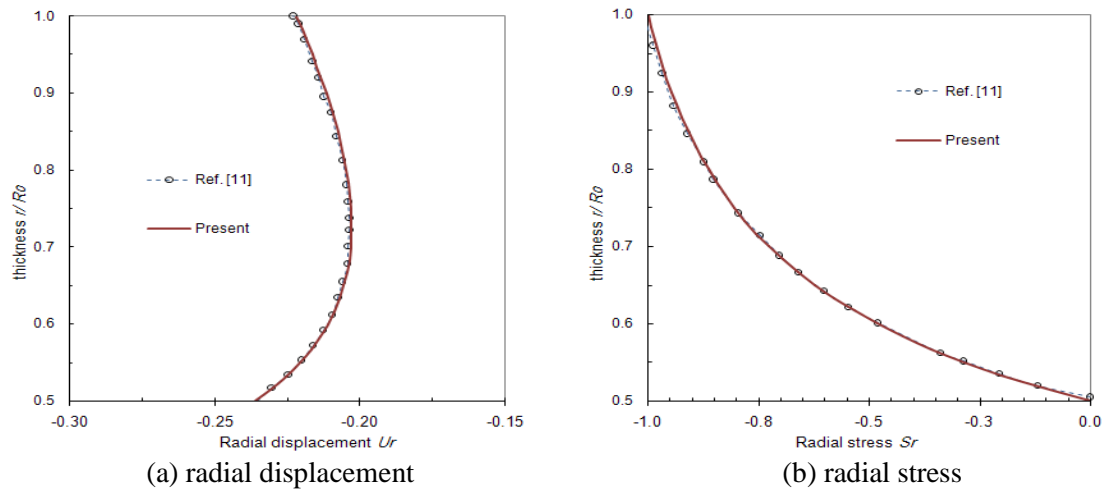


Figure 3 Comparison of thickness-wise variations, Case III

Table 1 Material properties of piezoelectric PZT-5

Elastic Constants, Gpa							
C_{11}	C_{12}	C_{13}	C_{22}	C_{23}	C_{33}	C_{44}	C_{55}
111.0	75.1	75.1	120.0	75.2	120.0	22.6	21.1
Piezoelectric Constants, C/m^2				Permittivity, $10^{-9}C^2/Nm^2$			
e_{11}	e_{12}	e_{13}	e_{35}	Δ_{11}			
15.78	-5.35	-5.35	12.7	1700			

Table 2 Comparison between results in the middle of shell thickness for Shell A

Electro-mechanical Loading	R_o/R_i	σ_r		σ_θ		ψ	
		present	Ref [7]	present	Ref [7]	present	Ref [7]
Case I	1.3	-0.439	-0.367	1.435	1.411	-0.338×10^{-5}	-0.412×10^{-5}
	2	-0.238	-0.185	0.311	0.307	-0.894×10^{-5}	-1.097×10^{-5}
	4	-0.041	-0.038	0.048	0.057	-1.256×10^{-5}	-1.528×10^{-5}
Case II	1.3	-0.972	-0.936	22.452	22.310	0.431	0.415
	2	-1.611	-1.538	6.377	6.294	0.329	0.325
	4	-1.274	-1.219	1.820	1.612	0.204	0.191
Case III	1.3	-1.194	-1.173	23.367	23.512	0.439	0.447
	2	-1.753	-1.681	6.814	6.735	0.332	0.333
	4	-1.205	-1.147	1.572	1.543	0.201	0.203
Case IV	1.3	-0.629	-0.642	-2.433	-2.521	0.203×10^{-5}	0.175×10^{-5}
	2	-0.783	-0.795	-1.230	-1.147	1.152×10^{-5}	1.129×10^{-5}
	4	-0.932	-0.928	-0.986	-0.815	6.337×10^{-5}	6.251×10^{-5}

Secondly, radial displacements of shell A corresponding to the above last three load cases are presented in Figures (4(a)) to (4(d)). As it is expected, the radial displacements for Case I are positive, while radial displacements of the other cases are negative, having incremental variation trends. Thin shell ($R_o/R_i= 1.3$) has a different deformation pattern from the thicker ones. It is inferred from Figures (4(c)) and (4(d)) that load Cases III and IV deliver very similar results, due to the shrinking effect of electric load. Next, the following spherical shell is investigated:

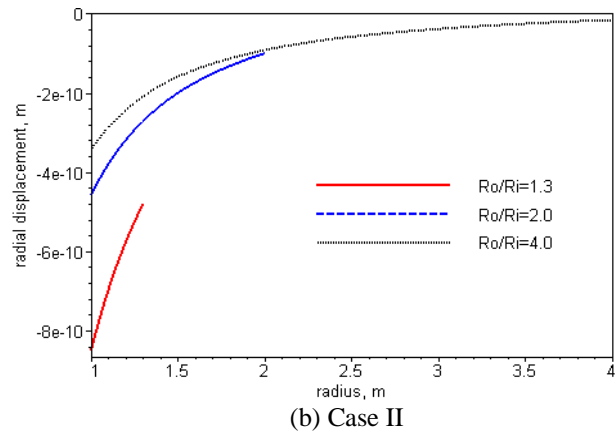
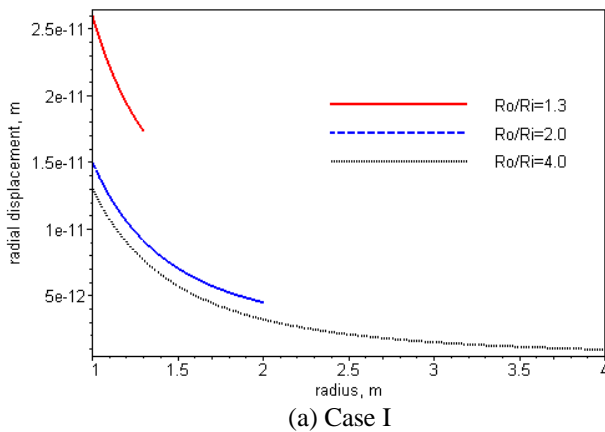
Shell B) FGPM made of piezoelectric ceramic PZT-4, which has been selected because of its technical applications. Mechanical and electrical properties of piezoelectric material, PZT_4 are tabulated in Table (3). Presented results are related to the five cases of different boundary conditions with aspect ratio $R_o/R_i= 1.3$. The numerical results are drawn in Figures (5) to (9), showing the variation of stresses, electric potential and displacement across the thickness of the FGPM sphere for different material inhomogeneity parameter n .

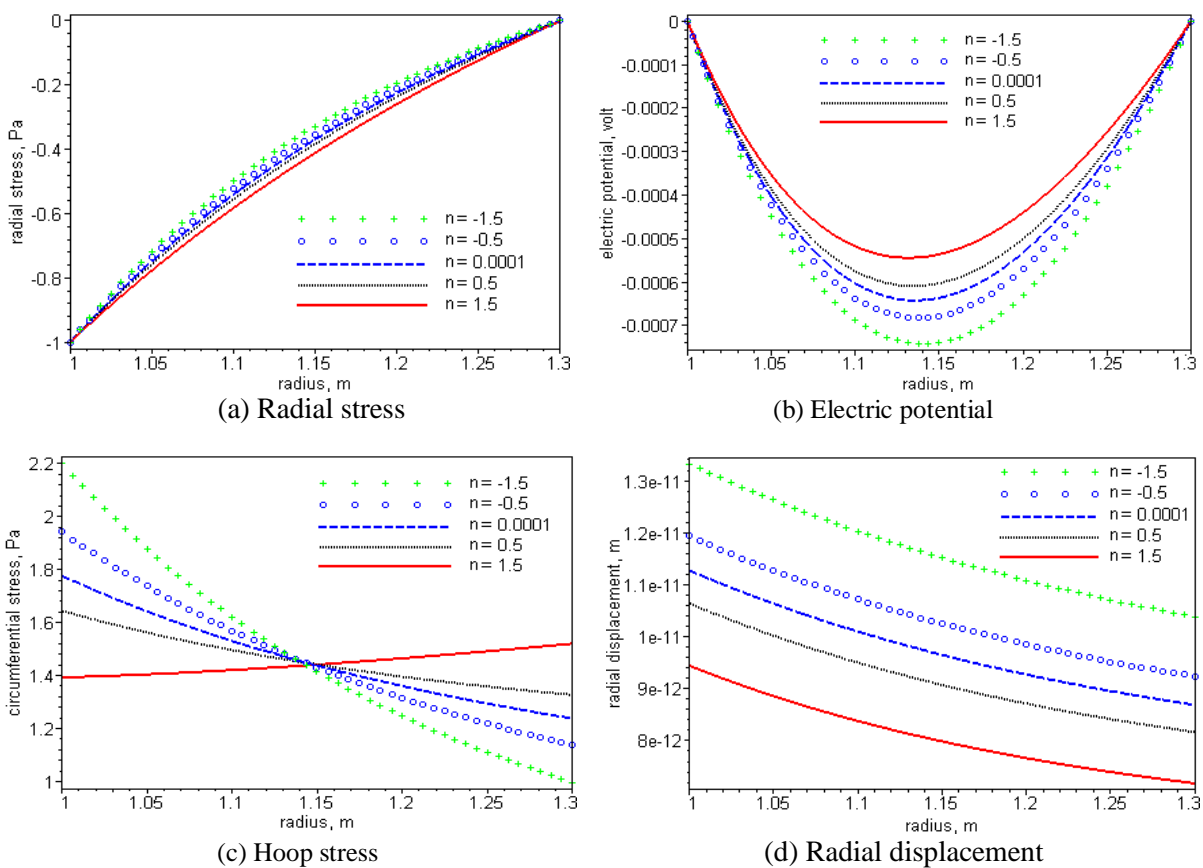
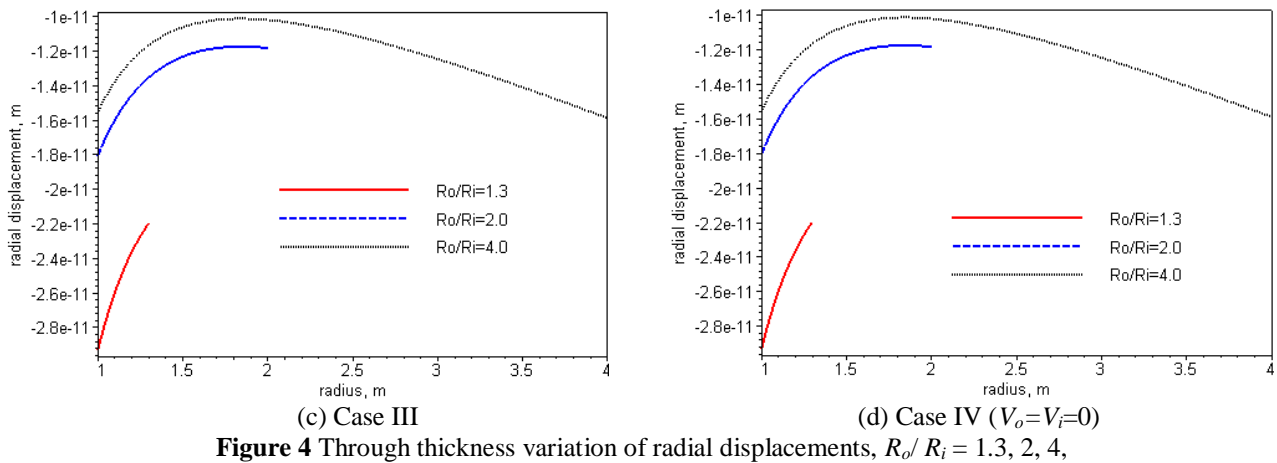
Table 3 Material properties of piezoelectric PZT-4

Elastic Constants, Gpa							
C_{11}	C_{12}	C_{13}	C_{22}	C_{23}	C_{33}	C_{44}	C_{55}
115.0	74.3	74.3	139.0	77.8	139.0	30.6	25.6
Piezoelectric Constants, C/m^2				Permittivity, $10^{-9}C^2/Nm^2$			
e_{11}	e_{12}	e_{13}	e_{35}	Δ_{11}	Δ_{22}		
15.1	-5.2	-5.2	12.3	3.87	4.91		

Case I

Results of the first case are illustrated in Figures (5). Radial stresses for different material inhomogeneity parameters n are shown in Figure (5(a)). Radial stresses satisfy the mechanical boundary conditions at the inner and outer surfaces of the FGPM sphere. The maximum absolute values of radial stresses belongs to a material identified by in-homogeneity parameter $n = 1.5$ the minimum absolute values of which belong to $n = -1.5$. In this case there is no imposed electric potential. However, the induced electric potentials for different material inhomogeneity parameters n are shown in Figure (5(b)). Electric potentials satisfy the grounded electrical boundary conditions at the inner and outer surfaces of the shell B. It is also obvious that higher induced electric potentials belong to higher absolute values of compressive radial stresses. Hoop stresses (Figure (5(c))) are highly tensile through thickness. Radial displacements are illustrated in Figure (5(d)) for all material properties. Displacements are positive throughout the thickness and they smoothly decrease from their maximum value at the inner surface to their minimum value at the outer surface of the shell B. Maximum values of displacements belong to $n= -1.5$ and minimum values belong to $n = 1.5$.





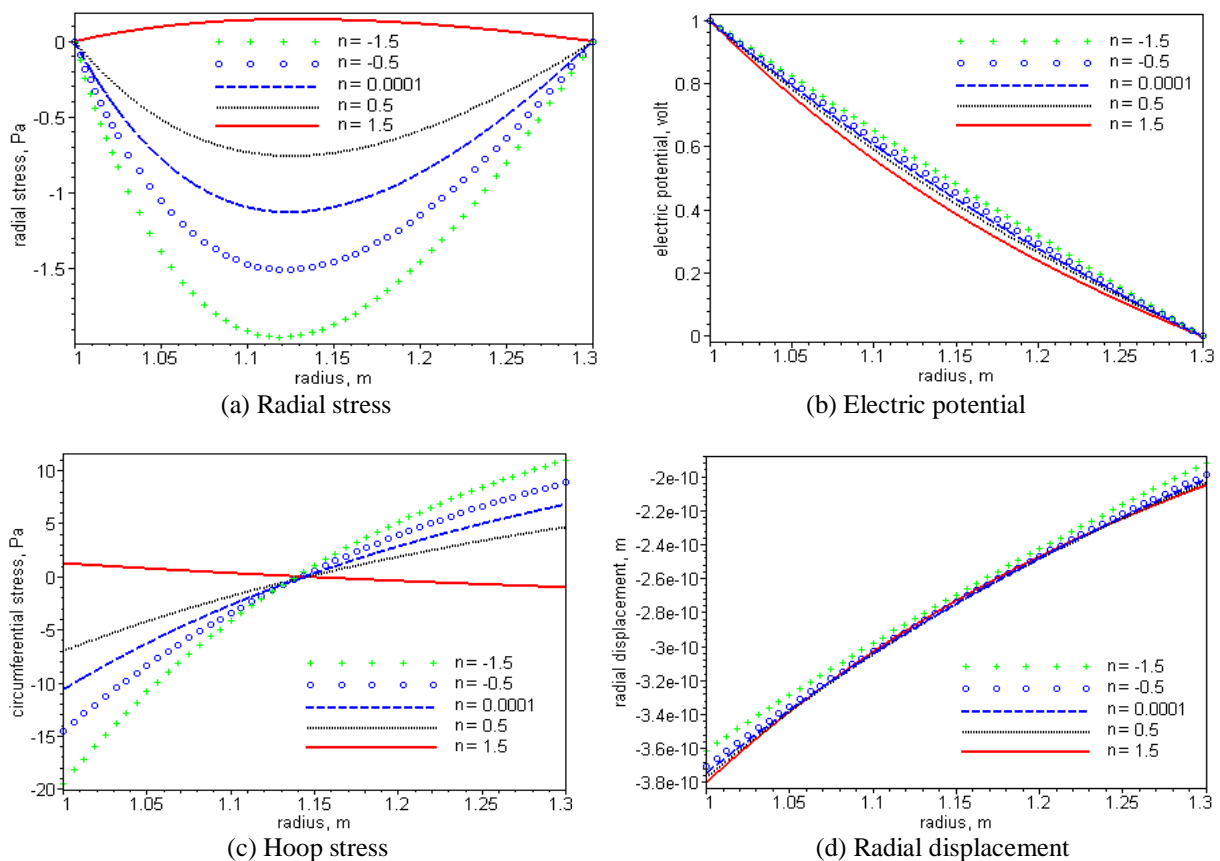
Case II

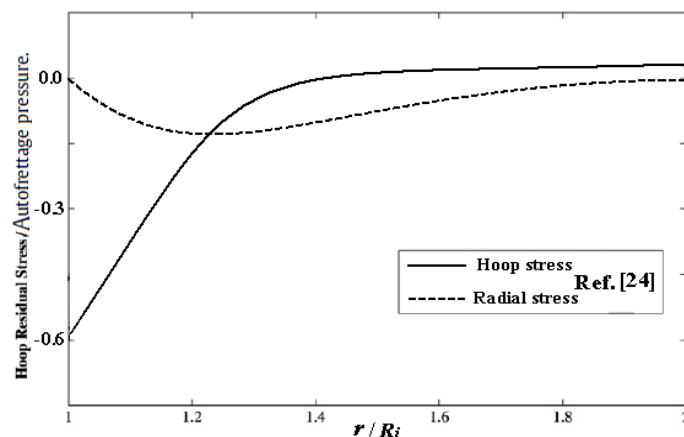
Results of the fully actuator case are illustrated in Figures (6(a)) to (6(e)). In which, there is no applied pressure at the inner and outer surfaces of the sphere however the induced compressive radial stresses satisfy the traction free mechanical boundary conditions. Interestingly, the maximum absolute values of the induced compressive radial stresses belong to the same maximum value of electric potential. In this case, the imposed electric potential satisfies the electrical boundary conditions at the inner and outer surfaces of the sphere. This means that the difference between electric potentials on inner and outer surfaces ($\Delta V = V_o - V_i$) are important rather than their individual values. That is, $V_o = 0, V_i = 1$ produces the same results as $V_o = -1, V_i = 0$. It is observed that the greater electric potentials belong to $n = -1.5$, while the smaller values of which belong to $n = 1.5$.

Circumferential induced stresses are both tensile and compressive throughout thickness for different material in-homogeneity parameters n . However, for negative parameters n the minimum values of circumferential stresses are located at the inner surface, while for positive parameters of n their minimum values are located at the outer surface of the FGPM sphere. This stress tends to vanish on the mid-radius for all parameters n . The induced radial displacement is negative across the thickness for all material parameters and about ten times larger than those of Case I (Figure 5(d)), in spite of which, the minimum values are located at the inner and their maximum values are at the outer surfaces of the shell B. It is observed from Fig. 6(e) that the overall behavior of induced radial and circumferential stresses locked in the sphere during the autofrettage process of spheres made of uniform material [25] are typically similar to thickness-wise stress distributions for load case II (Fig. 6(c)), in which radial stress caused by electric field vanishes at free surfaces of FGPM sphere. Circumferential induced stress is compressive on the inner radius and has a smaller tensile value on the outer radius. For negative parameters n , the minimum values of circumferential stress are located at the inner surface, while for positive parameters of n its minimum values are located at the outer surface of the FGPM sphere. This stress tends to vanish on the mid-radius for all parameters n .

Case III

Results of the third load case are illustrated in Figures (7(a)) to (7(d)). Radial stresses for different material in-homogeneity parameters n are shown in Figure (7(a)). Radial stresses satisfy the mechanical boundary conditions at the inner and outer surfaces of the shell B. The largest absolute values of radial stresses belong to a material identified by $n = -1.5$ and the smallest values of which belong to $n = 1.5$. In this case, there is no external electric potential; however, the induced electric potentials for different material in-homogeneity parameters n are shown in Figure (7(b)). Electric potentials satisfy the fully grounded electrical boundary conditions at the inner and outer surfaces of the shell B.





(e) Hoop and radial residual stress, [24]

Figure 6 Through thickness variation of results for five exponents n , $R_o/R_i = 1.3$, Case II, $\Delta V = -1$ volt

It is also clear that higher induced electric potentials correspond to those with larger absolute values of compressive radial stresses. Circumferential stresses are completely compressive across the thickness for different material in-homogeneity parameters n (Figure (7(c))). However, for negative parameters n the minimum values of circumferential stresses are located at the inner surface, while for positive ones their minimum values are at the outer surface of the FGPM sphere. It is interesting to see that the compressive circumferential stresses in this case is very similar to the induced circumferential stresses resulted from imposing an electric potential (Case II). Radial displacements are illustrated in Figure (7(d)) for all material properties. Displacements are again negative throughout the thickness and they smoothly change from their less value at the inner surface to their relatively constant values at the outer surface of the shell B. Maximum values of displacements belong to $n = -1.5$ and minimum values belong to $n = 1.5$.

Case IV

Case four is superposition of the Cases I and II. The results of this case are given in Figures (8(a)) to (8(d)). Radial stresses and the electric potentials satisfy the mechanical and electrical boundary conditions. A positive electric potential is applied on the internal surface, which is equal to imposing a negative electric potential on the external surface. The maximum compressive values of radial stresses belong to a material identified by $n = -1.5$ the minimum values of which belong to $n = 1.5$.

It is also clear that higher electric potentials correspond to those with less value of compressive radial stresses. Circumferential stress distribution is similar to those of Case II for different material in-homogeneity parameters n . However, for negative parameters n the minimum values of circumferential stresses located at the inner surface while for positive parameters c their minimum values located at the outer surface of the shell B.

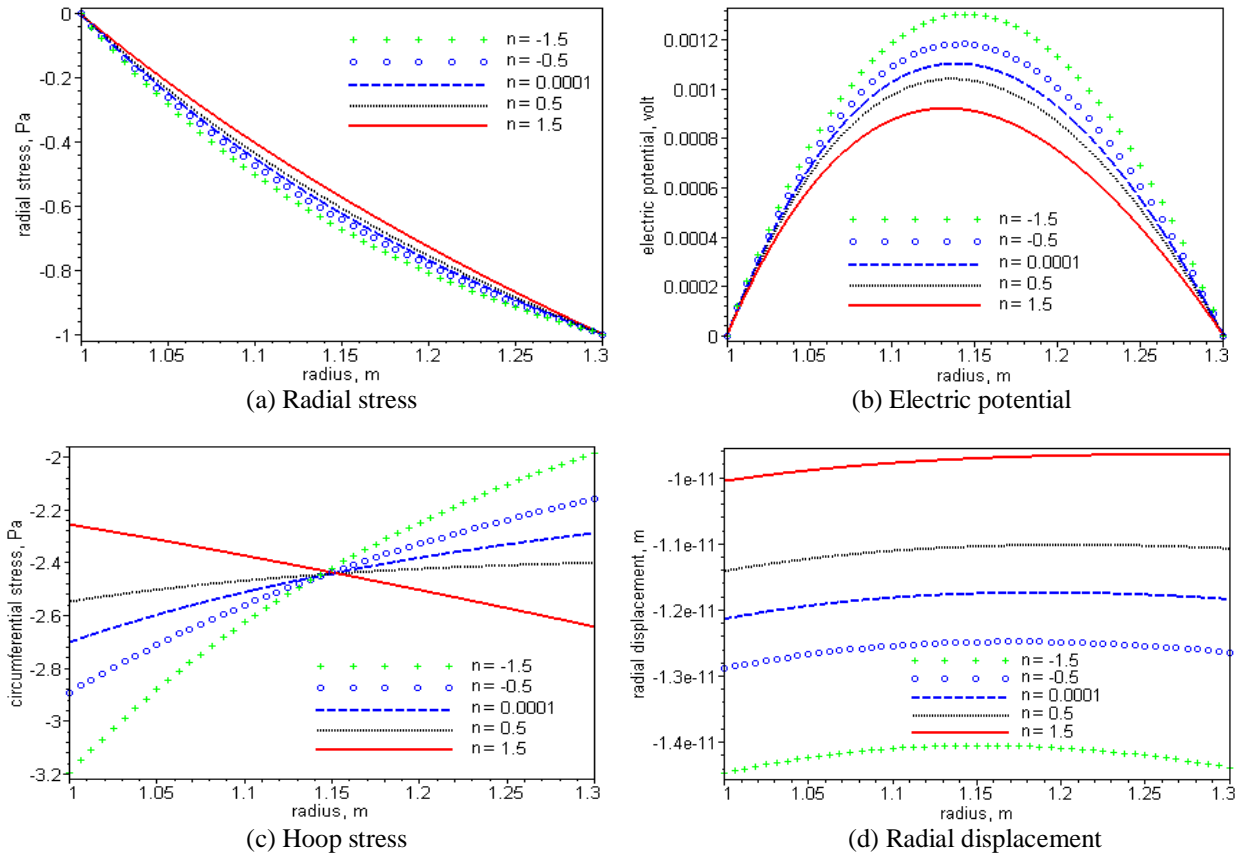


Figure 7 Through thickness variation of results for five exponents n , $R_o/R_i = 1.3$, Case III, $\Delta V = 0$ volt

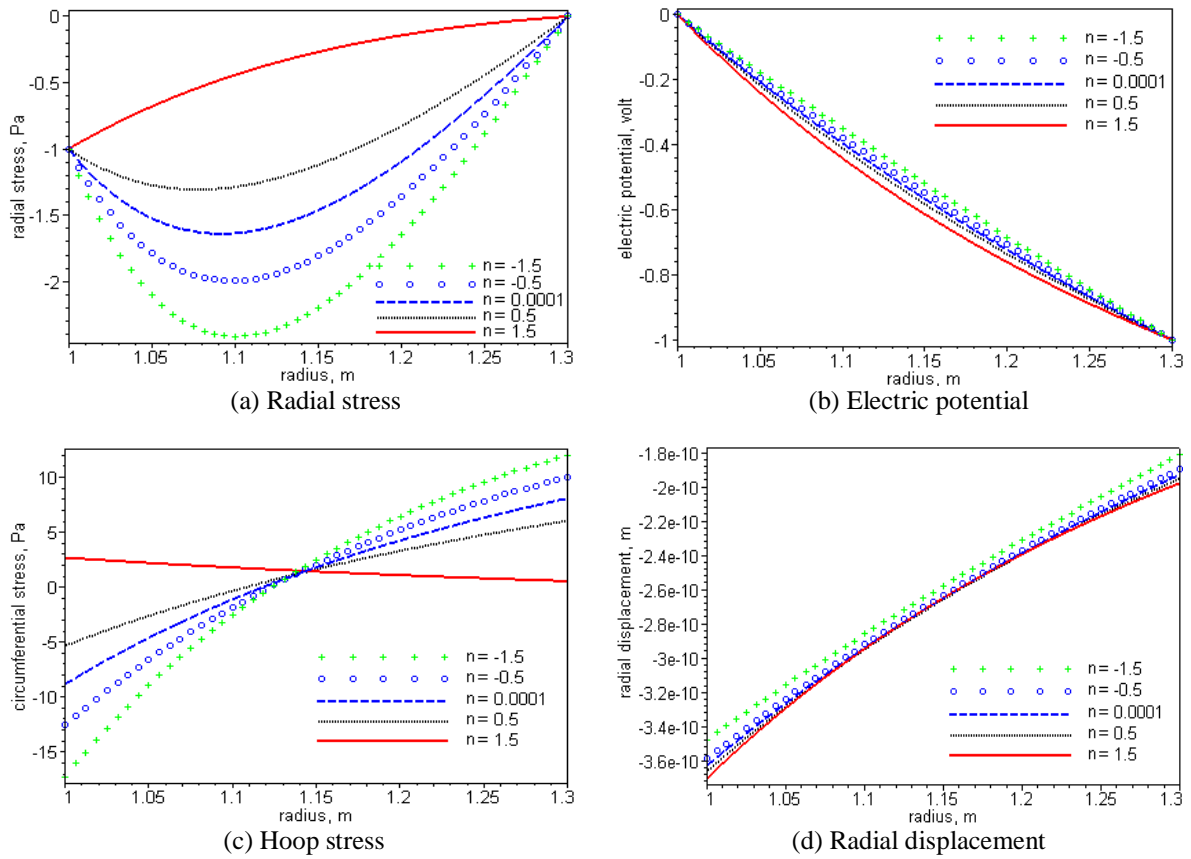


Figure 8 Through thickness variation of results for five exponents n , $R_o/R_i = 1.3$, Case IV, $\Delta V = -1$ volt

Radial displacement is negative across the thickness for all material parameters, resembling Figure (6(d)), except that the inward displacement is reduced slightly. Their minimum values located at the inner and their maximum values located at the outer surfaces of the shell B.

Case V

The aforementioned electrical loadings are not very practical, because it is more realistic to actuate the electrode installed on the external surface of the closed shell. Figure (9(a)) shows that although mechanical pressure is like the previous case, radial stress distribution has the opposite trend for different material parameters n . Similarly, electric potential demonstrates behaviours opposite to those given in Figure (8(b)). Circumferential stress distribution is similar to those of Case I for different material in-homogeneity parameters n .

However, a ten times increase is induced in this stress (Figure (9(c))), due to applied voltage. Despite all the previous cases, radial displacements are positive throughout the thickness and they vary closely from their maximum value on the inner surface to their minimum values on the outer surface. Comparing Figure (9(d)) with Figure (5(d)) infers that the positive electric load on the outer surface bucks the variation trend in radial displacement with regard to material exponent n , as well as intensifying the expansion of spherical shell B due to mechanical pressure, more than ten times and this might not be really desired in terms of shape control.

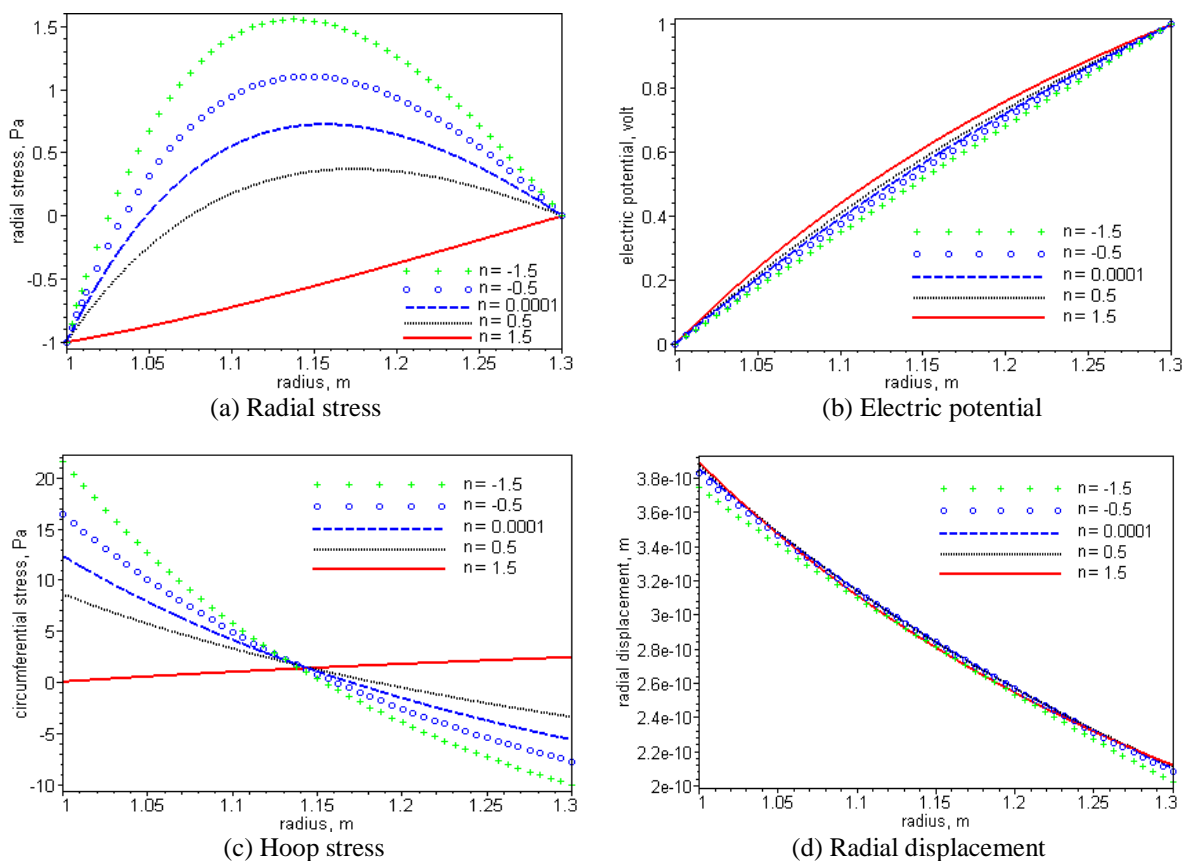


Figure 9 Through thickness variation of results for five exponents n , $R_o/R_i = 1.3$, Case V, $\Delta V = 1$ volt

5 Conclusion

An analytical approach is developed for the analysis of functionally graded piezoelectric spherical shells with piezoelectric properties subjected to different load. This study helps to deepen understanding of the behaviour of radially polarized FGPM smart structures. The effects of the geometrical parameters, boundary conditions and volume fraction exponent ' n ' on static behaviour of the FGPM sphere are demonstrated. Correlations between yielded results and existing solutions support the accuracy and versatility of developed formulations. Variation of stresses, electric potential and displacement of five sets of boundary conditions for different material in-homogeneity parameters n are plotted against radius. In general, radial stresses and electric potentials satisfy the mechanical and electrical boundary conditions at the inner and outer surfaces of the FGPM sphere. Higher absolute values of compressive radial stresses are associated with the higher induced electric potentials throughout the thickness in all cases. The other observations of this research can be outlined as follows:

1. The exact solution is only responsible to capture the correct through-thickness distributions of displacement. While, the constitutive equations are accountable for the overall accuracy of the stress components.
2. The present formulation is capable for static analysis of both thin and thick FGPM spheres, as well as preventing shear locking in thin shells.
3. Meaningful less amount of computational effort of the developed approach, with respect to the finite element method is witnessed.
4. It is seen that the compressive radial stress due to internal pressure tends to become tensile by imposing a negative electric potential, for shell with higher FGM exponents.
5. Electric excitation has a significant effect on the distribution of stress and displacement fields in a FGPM shell. So that, hoop stress becomes compressive on the internal radius and the amount of this stress resulted from internal pressure in FGPM sphere can be reduced (instead of being positive) by applying a proper amount of electric field as well as applying an external pressure, which can be substantial in terms of durability and surface fatigue crack growth in the shell. This scenario brings about very similar radial displacements for load Cases III and IV.

References

- [1] Crawley, E. F., "Intelligent Structures for Aerospace: a Technology Overview and Assessment", J. AIAA, Vol. 32, pp. 1689–1689, (1994).
- [2] Niino, A., and Maeda, S., "Recent Development Status of Functionally Gradient Materials", Int. J. ISI Vol. 30, pp. 699–703, (1990).
- [3] Yamada, K., Yamazaki, D., and Nakamura, K., "A Functionally Graded Piezoelectric Material Created by an Internal Temperature Gradient", Jpn J. Appl. Phys. Vol. 2, No. 40, pp. 49–52, (2001).
- [4] Chen, W. Q., Ding, H. J., and Liang, J., "The Exact Elastoelectric Field of a Rotating Piezoceramic Spherical Shell with a Functionally Graded Property", Int. J. Solids Struct., Vol. 38, pp. 7015–7027, (2001).
- [5] Lim, C. W., and He, L. H., "Exact Solution of a Compositionally Graded Piezoelectric Layer under Uniform Stretch Bending and Twisting", Int. J. Mech. Sci., Vol. 43, pp. 2479–2492, (2001).

- [6] Sinha, D.K., "Note on the Radial Deformation of a Piezoelectric, Polarized Spherical Shell with a Symmetrical Distribution", *J. Acoust. Soc.* Vol. 34, pp. 1073–1075, (1962).
- [7] Chen, W.Q., and Ding, H.J., "A State-space-based Stress Analysis of a Multilayered Spherical Shell with Spherical Isotropy", *J. Applied Mech.* Vol. 68, pp. 109–114, (2001).
- [8] Ghorbanpour, A., Golabi, S., and Saadatfar, M., "Stress and Electric Potential Fields in Piezoelectric Smart Spheres", *J. Mech. Sci. Technol.* Vol. 20, pp. 1920–1933, (2006).
- [9] Saadatfar, M., and Rastgoo, A., "Stress in Piezoelectric Hollow Sphere under Thermal Environment", *J. Mech. Sci. Technol.* Vol. 22, pp. 1460–1467, (2008).
- [10] Shao, Z. S., Fan, L. F., and Wang, T. J., "Analytical Solutions of Stresses in Functionally Graded Circular Hollow Cylinder with Finite Length", *J. Key Engng Mater.*, Vol. 261–263, pp. 651–656, (2004).
- [11] You, L.H., Zhang, J.J., and You, X.Y., "Elastic Analysis of Internally Pressurized Thick-walled Spherical Pressure Vessels of Functionally Graded Materials", *Int. J. Pres. Ves. Pip.* Vol. 82, pp. 347–354, (2005).
- [11] Ding, H.J., Wang, H.M., and Chen, W.Q., "Analytical Solution for a Non-homogeneous Isotropic Piezoelectric Hollow Sphere", *Arch. Appl. Mech.* Vol. 73, pp. 49–62, (2003).
- [12] Sladek, V., Sladek, J., and Zhang, Ch., "Transient Heat Conduction Analysis in Functionally Graded Materials by the Meshless Local Boundary Integral Equation Method", *Comput. Mater. Sci.* Vol. 28, pp. 494–504, (2003).
- [13] Sladek, J., Sladek, V., Sulek, P., and Saez, A., "Dynamic 3D Axisymmetric Problems in Continuously Non-homogeneous Piezoelectric Solids", *Int. J. Solids Struct.* Vol. 45, pp. 4523–4542, (2008).
- [14] Wang, H.M., and Xu, Z.X., "Effect of Material Inhomogeneity on Electromechanical Behaviors of Functionally Graded Piezoelectric Spherical Structures", *Comput. Mater. Sci.* Vol. 48, pp. 440–445, (2010).
- [15] Ghorbanpour, A., Salari, M., Khademizadeh, H., and Arefmanesh, A., "Magneto Thermoelastic Problems of FGM Spheres", *Arch. Appl. Mech.* Vol. 43, pp. 189–200, (2010).
- [16] Setoodeh, A.R., Tahani, M., and Selahi, E., "Hybrid Layerwise-differential Quadrature Transient Dynamic Analysis of Functionally Graded Axisymmetric Cylindrical Shells Subjected to Dynamic Pressure", *Composite Structures*, Vol. 93, pp. 2663–2670, (2011).
- [17] Ghorbanpour Arani, A., Kolahchi, R., Mosallaie Barzoki, A.A., and Loghman, A., "Electro-Thermo-mechanical Behaviors of FGPM Spheres using Analytical Method and ANSYS Software", *Appl. Math. Modeling*, Vol. 36, pp. 139–157, (2012).
- [18] Zill, D.G., "*A First Course in Differential Equations with Modeling Applications*", Brooks/Cole Publishing Company, California, (2001).

- [19] Sabzikar Boroujerdy, M., and Eslami, M. R., "Unsymmetrical Buckling of Piezo-FGM Shallow Clamped Spherical Shells under Thermal Loading", *Journal of Thermal Stresses*, Vol. 38, pp. 1290–1307, (2015).
- [20] Shakeri, M., Saviz, M.R., and Yas, M.H., "Three-Dimensional Elasticity Solution for Thick Laminated Cylinder with Piezoelectric Layer", *Iranian Journal of Mechanical Engineering, Transaction of ISME*, Vol.16, No.2, pp. 4-10, (2005).
- [21] Hafezalkotob, A., and Eslami, M. R., "Thermomechanical Buckling of Simply Supported Shallow FGM Spherical Shells with Temperature-dependent Material", *Iranian Journal of Mechanical Engineering, Transaction of ISME*, Vol. 11, pp. 39–65, (2010).
- [22] Institute of Electrical and Electronics Engineers, *Standard on Piezoelectricity, Std 176-1978 IEEE*, New York, (1978).
- [23] Reddy, J.N., "*Mechanics of Laminated Composite Plates and Shells: Theory and Analysis*", Boca Raton: CRC Press, (2004).
- [24] Tiersten, H.F., "*Linear Piezoelectric Plate Vibrations*", Plenum Press, New York, (1969).
- [25] Maleki, M., Farrahi, G.H., Haghpanah Jahromi, B., and Hosseinian, E., "Residual Stress Analysis of Auto frettagged Thick-walled Spherical Pressure Vessel", *Int. J. Pressure Vessels and Piping*, Vol. 87, pp. 396-401, (2010).

Nomenclature

$c_{ij}(r)$ = elastic constants at radius r
 C_{ij} = material constant for elastic constants
 $\{ED\}$ = electric displacement vector
 $e_{ij}(r)$ = piezoelectric constants at radius r
 e_{ij} = material constant for piezoelectric coefficients
 $\{EF\}$ = electric field vector
 $E_{ii}(r)$ = directional modulus of elasticity at radius r
 E = material constant for modulus of elasticity
 $G_{ij}(r)$ = shear modulus at radius r
 H = total shell thickness
 K_1, K_2, D and C' = constants in solutions of equations
 n = power-law exponent
 P_i and P_o = internal and external pressures
 R_i = inside radius,
 R_o = outside radius
 $u_r(r)$ = radial displacement
 V = distributed electric potential

Greek symbols

$\{\sigma\}$ = stress vector
 $\{\varepsilon\}$ = strain vector
 ψ = electric potential
 $\Delta_{ij}(r)$ = dielectric constants at radius r
 Δ_{ij} = material constant for dielectric constant

چکیده

براساس رویکرد حل الاستیسیته، مخزن کروی توخالی ساخته شده از ماده هدفمند پیزوالکتریک به صورت تحلیلی در راستای شعاعی بررسی شده است. تغییرات خواص مکانیکی برحسب نسبت حجمی به صورت تابع مدل توانی از مختصه راستای شعاعی کنترل می شوند. مخزن مزبور تحت فشار داخلی یا خارجی و بار الکتریکی گسترده با گرادیان پتانسیل الکتریکی مثبت یا منفی و به صورت مجزا و همزمان قرار گرفته است. مدل توانی برای در نظر گرفتن تغییرات خواص الکترومکانیکی به جز نسبت پواسون در امتداد ضخامت می باشد. برای تقارن محوری، معادلات سه بعدی حاکم به یک معادله دیفرانسیل غیر خطی کوشی اویلر برحسب جابجایی شعاعی تبدیل می شوند. این معادله بصورت تحلیلی حل شده است. حل عمومی معادله دیفرانسیل بصورت تابع توانی و حل خصوصی متفاوت از کارهای قبلی چاپ شده می باشد.

با نوشتن پنج شرط مرزی مختلف و اعمال آنها به حل بدست آمده برای معادله مذکور، یک دستگاه معادلات جبری برحسب چهار ثابت مجهول بدست می آید. بدین ترتیب میدان جابجایی و تنش در کره حل می شود. پاسخ استاتیکی کره با مواد پیزوالکتریک همگن و ابعاد هندسی مختلف به بارهای مکانیکی و الکتریکی جهت مقایسه با مراجع موجود استفاده شده است. سپس پاسخ کره با توان های تابع هدفمندی و ابعاد هندسی مختلف تحت بارهای مکانیکی و الکتریکی متنوع بررسی شده است. تنشهای بوجود آمده در اثر بار الکتریکی قابل مقایسه با تنشهای پسماند محبوس در یک کره ساخته شده از مواد غیر پیزوالکتریک و همگن می باشد.